Environmental Pollution 193 (2014) 88–93

Contents lists available at ScienceDirect

Environmental Pollution

journal homepage: www.elsevier.com/locate/envpol

Decreasing effect and mechanism of $FeSO_4$ seed particles on secondary organic aerosol in α-pinene photooxidation

Biwu Chu [a, b], Yongchun Liu [a, d], Junhua Li [b], Hideto Takekawa [c], John Liggio [d], Shao-Meng Li [d], Jingkun Jiang [b], Jiming Hao [b], Hong He [a, *]

[a] State Key Joint Laboratory of Environment Simulation and Pollution Control, Research Center for Eco-Environmental Sciences, Chinese Academy of Sciences, Beijing 100085, China
[b] State Key Joint Laboratory of Environment Simulation and Pollution Control, School of Environment, Tsinghua University, Beijing 100084, China
[c] Toyota Central Research and Development Laboratory, Nagakute, Aichi 480-1192, Japan
[d] Air Quality Research Division, Environment Canada, Toronto, Ontario, Canada

ARTICLE INFO

Article history:
Received 9 April 2014
Received in revised form
11 June 2014
Accepted 12 June 2014
Available online 9 July 2014

Keywords:
Secondary organic aerosol
$FeSO_4$ seed particle
α-Pinene
Decreasing effect
Relative humidity

ABSTRACT

α-Pinene/NO_x and α-pinene/HONO photooxidation experiments at varying humidity were conducted in smog chambers in the presence or absence of $FeSO_4$ seed particles. $FeSO_4$ seed particles decrease SOA mass as long as water was present on the seed particle surface, but $FeSO_4$ seed particles have no decreasing effect on SOA under dryer conditions at 12% relative humidity (RH). The decreasing effect of $FeSO_4$ seed particles on the SOA mass is proposed to be related to oxidation processes in the surface layer of water on the seed particles. Free radicals, including OH, can be formed from catalytic cycling of Fe^{2+} and Fe^{3+} in the aqueous phase. These radicals can react further with the organic products of α-pinene oxidation on the seed particles. The oxidation may lead to formation of smaller molecules which have higher saturation vapor pressures and favor repartitioning to the gas phase, and therefore, reduces SOA mass.

1. Introduction

Secondary organic aerosol (SOA) is an important component of fine particles in both urban and rural atmosphere. Its influence on human health (Kaiser, 2005), visibility degradation (Cheng et al., 2011), and climate change (Satheesh and Moorthy, 2005) has drawn increased attention. Numerous factors can influence the formation of SOA. These factors include temperature (Hessberg et al., 2009; Jonsson et al., 2008; Qi et al., 2010; Takekawa et al., 2003), relative humidity (RH) (Healy et al., 2009; Prisle et al., 2010; Tillmann et al., 2010; Zhang et al., 2011), hydrocarbon to NO_x ratio (Song et al., 2005), radiation (Liu et al., 2009; Warren et al., 2008), and pre-existing particles (Chu et al., 2012; Czoschke et al., 2003; Jang et al., 2002; Liggio and Li, 2008; Lu et al., 2009).

The effects of RH on SOA formation are complicated. Increased RH was found to either enhance (Healy et al., 2009; Tillmann et al., 2010) or reduce SOA formation (Zhang et al., 2011). Although physical uptake of water is negligible (Tillmann et al., 2010), one way RH increases SOA yields is through enhanced HONO formation in the presence of NO_x, which leads to increased concentration of OH radical (Healy et al., 2009). Increased concentration of OH radical will in turn enhance the oxidation of volatile organic compounds (VOCs), influence organic product distributions and increase SOA formation. Recently, model, laboratory studies and field observations have suggested that aqueous-phase chemistry in cloud and particle water contributed significantly to SOA formation, which was well summarized by Ervens et al. (2011). RH is also believed to influence gas/particle partitioning (Healy et al., 2009); increased RH causes more dicarbonyls and other water soluble oxygenated VOCs to partition into the particulate phase. Conversely, high RH can inhibit SOA formation due to its suppression of condensation reactions in the particle phase (Liggio and Li, 2008; Liggio et al., 2007; Nguyen et al., 2011), of which water is a product. For example, particle-phase organic esterification, which is favored to occur at low RH conditions, is proposed to contribute to SOA mass (Liggio et al., 2007; Zhang et al., 2011), but will be suppressed at high RH.

The effects of preexisting particles or seed particles on SOA formation remains uncertain due to the diversity of particles in air and the complexity of heterogeneous reactions. In laboratory studies, seed particles were usually used to facilitate initial

* Corresponding author.
E-mail address: honghe@rcees.ac.cn (H. He).

http://dx.doi.org/10.1016/j.envpol.2014.06.018

condensation when simulating SOA formation in smog chambers (Odum et al., 1996). In the past few decades, many have observed that the SOA formation is enhanced in the presence of acid seed particles (i.e. $(NH_4)_2SO_4$ and H_2SO_4) (Jang et al., 2002; Kroll et al., 2007; Liggio et al., 2005; Lu et al., 2009). The enhancement effect is believed to be rooted in particle-phase heterogeneous reactions (Jang et al., 2002), which can be catalyzed by the presence of acidic seed particles. These acid-catalyzed reactions lead to the formation of high-molecular weight and low-volatility species (e.g. oligomers), and thus increase SOA yields (Czoschke et al., 2003; Hallquist et al., 2009; Liggio and Li, 2008). While acidic seed particles have been extensively studied, few report the effect of other inorganic seed particles on SOA formation (Chu et al., 2013; Liu et al., 2013; Lu et al., 2008). Iron is one of the most abundant transition metals in the atmosphere (Cakmak et al., 2014; He et al., 2001) and exists in various chemical forms. Fe(II) could be a major contributor to total atmospheric iron under certain atmospheric conditions (Zhuang et al., 1992). In urban sites, the concentrations of water soluble Fe(II) in fine particle ($PM_{2.5}$) varied from very low to approximately 300–400 ng m^{-3}, lasting a few hours (Oakes et al., 2010). Particulate iron has important catalytic effects on reactions through Fenton-like chemistry that produces reactive oxygen species (ROS), including hydroxyl radicals, hydrogen peroxide, and oxidized organic species (Tao et al., 2003; Vidrio et al., 2008; Zhang et al., 2008). These ROS may influence SOA formation. In our previous work, preliminary results indicated that $FeSO_4$ seed particles had a significant suppression effect on SOA formation (Chu et al., 2012), yet a clear understanding of the cause of this effect was elusive.

In the current work, new smog chamber experiments were performed to further understand the effect of RH and metallic seed particles simultaneously, on SOA formation. In varying the humidity in the presence of $FeSO_4$ seed particles, further constraints on the mechanism of SOA suppression by metallic species can derived. The oxidation state of SOA was analyzed to obtain an improved understanding of the effect of $FeSO_4$ seed particles on SOA formation.

2. Materials and methods

2.1. Experimental system

Two smog chambers were used in this study. The first is a 2 m^3 cuboid reactor constructed with 50 μm-thick FEP-Teflon film (Toray Industries, Inc. Japan), with a surface-to-volume ratio of 5 m^{-1}. The chamber was described in detail in Wu et al. (2007). A temperature controlled enclosure (Escpec SEWT-Z-120) provides a constant temperature between 10 °C and 30 °C (±0.5 °C) and 40 black lights (GE F40T12/BLB, peak intensity at 365 nm) provide irradiation during the experiments. The hydrocarbon concentration is measured by a gas chromatograph (GC, Beifen SP-3420) equipped with a DB-5 column (30 m × 0.53 mm × 1.5 mm, Dikma) and flame ionization detector (FID), while NO_x and O_3 are monitored by a NO_x analyzer (Thermo Environmental Instruments, Model 42C) and an O_3 analyzer (Thermo Environmental Instruments, Model 49C), respectively. A scanning mobility particle sizer (SMPS, TSI 3936) is used to measure the size distribution of particulate matter (PM) in the chamber, and also used to estimate the volume and mass concentration.

The second chamber has been described by Bunce et al. (1997). This chamber is a 9 m^3 cylindrical reactor, with a surface-to-volume ratio of 2.7 m^{-1}. The reactor was irradiated by Phillips fluorescent UV-A and Sylvania black light lamps. The chamber was connected to a proton transfer reaction mass spectrometer (PTR-MS, IONICON Analytik) to measure gas phase organic compounds and an O_3 monitor (2B Technologies) to measure ozone. In addition, particle size distribution and chemical composition were measured by an SMPS and an aerosol mass spectrometer (AMS, Aerodyne Research, Inc. C-ToF-AMS). A negative-ion proton-transfer chemical-ionization mass spectrometry (NI-PT-CIMS) was used to evaluate the concentration of HONO in the experiments. The NI-PT-CIMS was described in detail elsewhere (Veres et al., 2008).

In both chambers, α-pinene was introduced into the chamber via its evaporation into a flow of zero air. HONO was generated by passing HCl gas through a tube filled with $NaNO_2$ salt granules similarly as described by Roberts et al. (2010). NO_x was introduced into the chamber from standard concentration cylinders (200 ppm) and further diluted. Seed particles were generated by atomizing 1 g L^{-1} $FeSO_4$ or $(NH_4)_2SO_4$ salt solutions using a constant output atomizer (TSI Model 3076). After removing water in a diffusion dryer (TSI Model 3062) and achieving an equilibrium charge distribution in a neutralizer (TSI Model 3077), the seed particles are carried and then flushed into the chamber by purified dry air in the smaller chamber. While in the experiments performed in the larger chamber, a differential mobility analyzer (DMA, TSI Model 3081) is used to produce monodispersed particles for input into the chamber.

2.2. SOA yield calculation

Since particles deposit on the Teflon film during the experiments, the particle concentrations measured by SMPS must be corrected for this depositional loss. Deposition rate is dependent upon particle size. Takekawa et al. (2003) estimated the particle deposition rate constant ($k(d_p)$, h^{-1}) was a four-parameter function of particle diameter (d_p, nm), as shown in Equation (1):

$$k(d_p) = a \times d_p^b + c \times d_p^d \quad (1)$$

The resulting $k(d_p)$ values for different d_p (40–700 nm) were determined by monitoring the particle number decay under dark conditions at low initial concentrations (<1000 particles cm^{-3}) to avoid serious coagulation. In the 2 m^3 chamber, the optimized values of parameter a, b, c, and d are calculated to be 6.46×10^{-7}, 1.78, 13.2, and −0.957, respectively. These values are valid for the conditions of three RHs of the experiments. In the 9 m^3 chamber, the particle deposition rate is significantly slower, and the optimized values of parameter a, b, c, and d were calculated to be 7.87×10^{-8}, 1.93, 1.33, and −1.228, respectively. In this study, the amount of aerosol mass added because of wall loss accounted for an average of approximately 5% total SOA mass from α-pinene. We believe the uncertainty resulting from wall deposition does not yield significant differences among the experiments.

The volume concentration of the generated SOA was derived after the wall deposition correction and deducting seed particles, by assuming the particles were spherical and nonporous. A unit density (1.0 g cm^{-3}) is used to calculate SOA mass concentrations, following the approach used in Takekawa et al. (2003), Verheggen et al. (2007) and our previous study (Chu et al., 2012). Then, SOA yield (Y), the ratio of the generated organic aerosol concentration (M_o) to the amount of reacted hydrocarbon concentration (ΔHC), is used to represent the aerosol formation potential of the hydrocarbon (Pandis et al., 1992).

2.3. Experimental conditions

Experiments with a matrix of different conditions of various concentrations of α-pinene, seed particle and RH were conducted in the 2 m^3 chamber. Detailed experimental conditions of these experiments, including relative humidity (RH), and initial concentrations of α-pinene ([α-pinene]), $FeSO_4$ seed particle ([$FeSO_4$]), and NO_x ([NO] and [NO_x–NO]) are listed in Table 1. The generated SOA mass (M_o) and SOA yield (Y) are also listed in Table 1. Photooxidation of two different initial concentrations of α-pinene (P1 and P2) were investigated. Seed-introduced experiments were carried out in the presence of $FeSO_4$ seed particles ("FS"), while the remaining experiments were seed-free experiments ("N"). Experiments were performed at a same temperature (30 °C) but three different RHs (i.e. 12%, 50% and 80%).

Additional four experiments were conducted in the 9 m^3 cylindrical reactor. Initial experimental conditions of these experiments are listed in Table 2. In these experiments, low concentrations of α-pinene were oxidized by OH radical, which was generated from the photolysis of the introduced HONO. The initial HONO concentration (9 ppb) was measured by the NI-PT-CIMS. In a controlled experiment with a same concentration of HONO, the concentration of the generated OH radical in the reactor was calculated to be $(2.8–4.6) \times 10^6$ molecule cm^{-3} by measuring the decay of methanol using the PTR-MS. Similar initial mass concentration of $FeSO_4$ or $(NH_4)_2SO_4$ seed particle ([$FeSO_4$] or [$(NH_4)_2SO_4$]) were introduced in the experiments listed in Table 2. Two RHs (12% and 50%) were designed to investigate their effects on SOA formation, which was measured by both the SMPS and the AMS.

Table 1
Experimental conditions and SOA formation in α-pinene/NO_x photooxidation. All the experiments were carried at 30 °C. SOA formation is indicated by generated SOA mass (M_o) and SOA yield (Y).

Experiment no.	RH (%)	[α-pinene] (ppm)	[$FeSO_4$] (μm^3 cm^{-3})	[NO] (ppb)	[NO_x–NO] (ppb)	M_o (μg m^{-3})	Y (%)
P1-N(50%)	50	0.21	0.0	53	51	96	8.4
P1-N(12%)	12	0.21	0.0	53	53	120	10.4
P1-N(80%)	80	0.20	0.0	54	49	130	12.0
P1-FS(50%)	50	0.21	10.4	52	55	41	3.6
P1-FS(12%)	12	0.21	10.3	49	57	114	10.2
P1-FS(80%)	80	0.21	9.8	51	56	60	5.2
P2-N(50%)	50	0.31	0.0	78	74	185	11.0
P2-N(12%)	12	0.31	0.0	81	75	210	12.3
P2-N(80%)	80	0.30	0.0	75	79	229	13.9
P2-FS(50%)	50	0.31	10.6	73	80	85	5.1
P2-FS(12%)	12	0.31	10.2	77	80	222	13.2
P2-FS(80%)	80	0.31	11.4	74	77	121	7.2

Table 2
Experimental conditions and SOA formation in α-pinene/HONO photooxidation. All the experiments were carried at 28 °C, with an initial concentration of HONO about 9 ppb. SOA formation is indicated by generated SOA mass (M_o) and SOA yield (Y).

Experiment no.	RH (%)	[α-pinene] (ppb)	[$FeSO_4$] ($\mu m^3\ cm^{-3}$)	[$(NH_4)_2SO_4$] ($\mu m^3\ cm^{-3}$)	M_o ($\mu g\ m^{-3}$)	Y (%)
FS(50%)	50	10.0	2.2		2.9	5.7
AS(50%)	50	11.7		1.8	9.3	23.4
FS(12%)	12	9.7	2.0		5.0	10.9
AS(12%)	12	8.1		1.7	5.9	15.1

In this study, the initial concentrations of reactants were higher than those present in the atmosphere. This served to generate high SOA concentrations and reduce relative error due to particle deposition. In the small chamber, the ratios of total VOCs to NO_x were similar as the ambient atmosphere since only one hydrocarbon was used in the experiments. In the large chamber, the ratios of α-pinene to HONO and the OH radical concentrations were comparable to the ambient atmosphere.

3. Results and discussions

3.1. Effects of $FeSO_4$ seed particles on SOA formation at different humidities

The effect of $FeSO_4$ seed particles on SOA formation depends on humidities. In Fig. 1, "$PM_{corrected} - PM_0$" presents the net organic aerosol formed, where $PM_{corrected}$ is calculated from the measured mass concentration of particles after correction for wall deposit losses as described previously, while PM_0 is the initial mass concentrations of seed particles. SOA yields followed quite similar trends with the PM concentrations since almost all the α-pinene was consumed in about an hour in the experiments. As demonstrated in Fig. 1, at 50% and 80% RH, particle concentrations in experiments with $FeSO_4$ seed particles are lower than in the corresponding seed-free experiments under otherwise identical initial conditions. These results indicate that there is a decreasing effect on SOA mass caused by the $FeSO_4$ seed particles under both RH conditions. However, this effect disappeared in experiments when RH dropped to 12%. Particle mass concentrations in experiments with $FeSO_4$ seed particles introduced at low RH, i.e. Experiments P1-FS(12%) and P2-FS(12%), were similar to those in the corresponding seed-free experiments, i.e. Experiments P1-N(12%) and P2-N(12%).

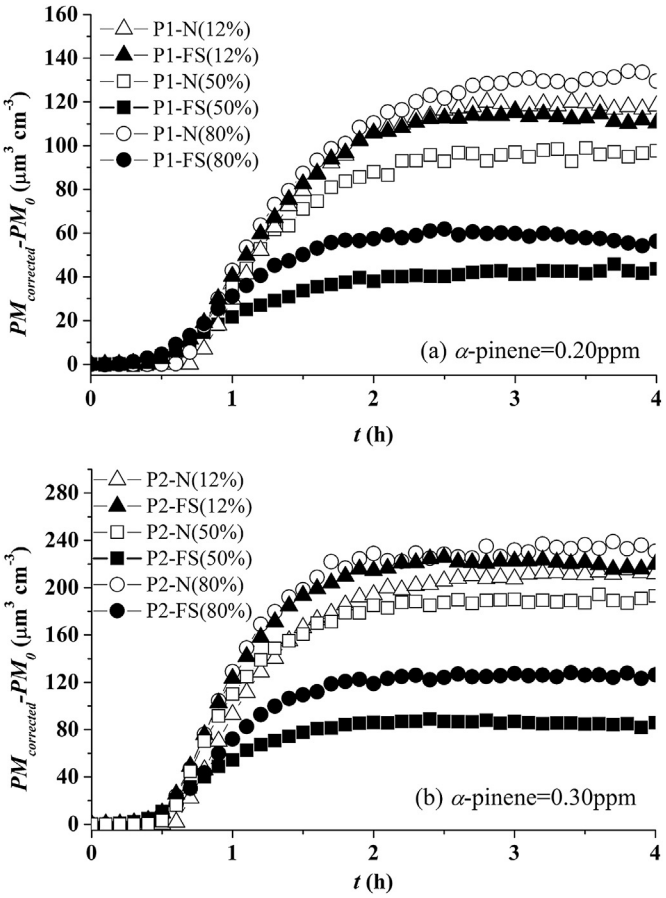

Fig. 1. Time variations of SOA concentration in α-pinene/NO_x photooxidation with/without $FeSO_4$ seed particles at different RHs.

3.2. Hygroscopic growth properties of $FeSO_4$ particles

One possible reason resulting in $FeSO_4$ seed particles having different effects on SOA formation at different RHs is that the seed particles have significant hygroscopic growth properties. Significantly different surface areas and volumes for SOA uptake and reactions are provided under different RHs on the seed particles. To demonstrate this possibility, the hygroscopic growth curve of $FeSO_4$ particles was measured using a hygroscopic tandem differential mobility analyzer (HTDMA) system, which was described elsewhere (Chu et al., 2014). The hygroscopic growth factor (Gf) was determined as:

$$Gf = d_p/d_{p0} \quad (2)$$

where d_{p0} is the diameter of the initial dry particles (RH<10%), and d_p is the diameter of the humidified particles after absorbing water in a TDMA at a given RH, respectively. $FeSO_4$ particles with d_{p0} of 100 nm were selected to measure their hygroscopic growth. As indicated in Fig. 2, $FeSO_4$ particles have no detectable hygroscopic growth when RH is below 30%, but begin to absorb water and grow when RH increases to approximately 40%. The Gf of $FeSO_4$ particle then increases nearly linearly with increasing RH from 40% to 80%. This growth curve indicates that $FeSO_4$ seed particles were dry in experiments at 12% RH, while there was a significant water uptake on $FeSO_4$ seed particle in experiments at RH of 50% and 80%. This suggests that the decreasing effect of $FeSO_4$ seed particles on SOA mass may be related to the amount of water present in the particle phase.

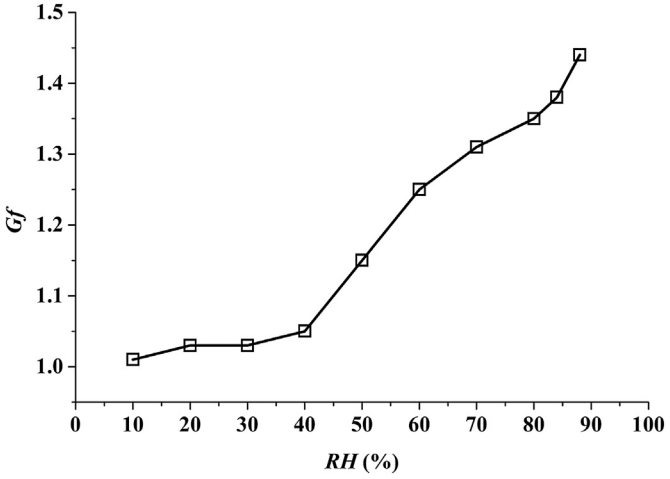

Fig. 2. Hygroscopic growth curve of FeSO4 particles. The hygroscopic growth factor (Gf) was measured using particles with initial dry diameter (d_{p0}) of 100 nm.

3.3. Decreasing mechanism of $FeSO_4$ seed particles on SOA formation

Deguillaume et al. (2005) gave a thorough review of the possible aqueous phase chemistry of Fe^{2+} and Fe^{3+} involving radicals and peroxides in the aqueous phase. Free radicals, including OH, can be formed from catalytic cycling of Fe^{2+} and Fe^{3+} in the aqueous phase. Both Fenton reaction (Ervens et al., 2003) and photolysis of Fe^{3+} complexes (Faust and Hoigne, 1990) in aqueous phase produce OH radical. As described by Deguillaume et al. (2005) and references therein, the importance of the Fenton reaction and photolysis of Fe^{3+} in the production of OH radicals in solution is still under debate and dependent on many factors, such as iron concentrations and pH value. In this study, the high concentration of iron may provide a favorable condition for the generation of free radicals. These radicals can react further with the organic mass on the seed particles from partitioning of the gas phase products of α-pinene oxidation, breaking them down into smaller molecules and resulting in loss of organic species from SOA. OH radicals from gas phase may also be taken up into the aqueous phase and react with organics, but it is estimated to be negligible compare to the OH production based on Fenton reaction there.

The effects of $FeSO_4$ seed particles on SOA formation were further investigated in experiments in the 9 m^3 chamber at concentrations of α-pinene a factor of 10–30 times lower than in experiments conducted in the smaller chamber. Control experiments using $(NH_4)_2SO_4$ were also conducted under similar conditions in the larger chamber. The time variation of SOA formation (represented as Organics/SO_4) is given in Fig. 3(a). SO_4 normalization removes particle wall loss effects (Liggio and Li, 2013). The SOA yields were separately determined based on the SMPS and AMS results, which are shown in the inner picture in Fig. 3(a). SOA yields in Fig. 3, calculated from the SMPS data are lower than the AMS results likely due to the unit density (1.0 g cm^{-3}) which was assumed to derive SOA mass concentrations. The ratio of the AMS to SMPS results indicates that the density of the formed SOA is approximately 1.4 g cm^{-3}. As demonstrated in Fig. 3, the use of $(NH_4)_2SO_4$ seed particles lead to higher SOA formation than $FeSO_4$ seed particles at both 12% and 50% RH. This difference may be attributed to both the decreasing effect of $FeSO_4$ seed particles and an enhancement effect of $(NH_4)_2SO_4$ seed particles (Kroll et al., 2007; Lu et al., 2009; Zhao et al., 2008) on SOA formation. At 50% RH, the SOA was a factor 2.5 higher on the $(NH_4)_2SO_4$ seed particles than on the $FeSO_4$ seed particles. At 12% RH, this difference is much smaller at about 20%. As demonstrated in Fig. 3, SOA yields were similar at 12% and 50% RH on the $(NH_4)_2SO_4$ seed particles. While on the $FeSO_4$ seed particles, SOA yield was a factor 1.8 higher at 12% RH than at 50% RH. This is consistent with the experimental results in the smaller chamber described above, in which we found $FeSO_4$ seed particles decrease SOA mass at 50% RH but had no decreasing effect on SOA formation at 12% RH.

The mechanism for the decreasing effect of $FeSO_4$ seed particles on SOA mass was further explored with an AMS, which was used to measure the chemical composition of the particles. Time variations for the ratio of two mass fragments, with mass to charge ratio (m/z) 44 and m/z 43, are shown in Fig. 3(b). The mass fragment m/z 44 results from highly oxidized organic components, while m/z 43 is from less oxidized organic components (Liggio et al., 2010; Ng et al., 2010). The relative strength of these two mass fragments has been used to infer the degree of oxidation of the SOA. In the first few minutes of all the four experiments, ratio of m/z 44 to m/z 43 decreased to a minimum value. This means that more oxidized organic components were taken up initially, followed by the less oxidized components. After the minimum in the ratio was reached, there was a consistent increase over time as the experiments

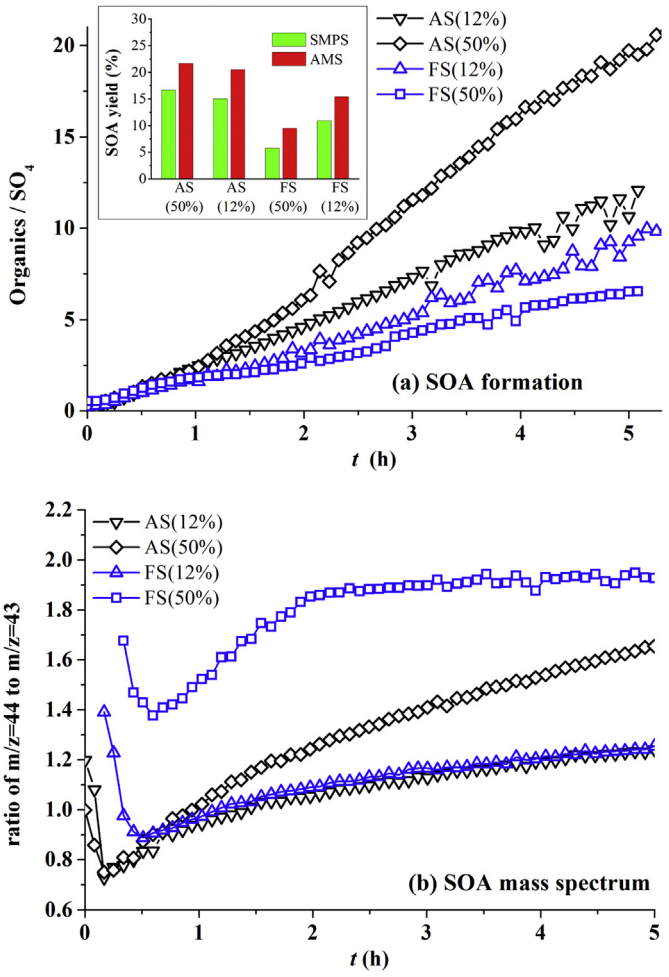

Fig. 3. SOA formation (a) and SOA mass spectrum properties (b) from photooxidation of α-pinene/HONO with different RH in the presence of sulfate seed particles.

continued. This indicated that more oxygenated SOA, compare to the average oxidation level of gas phase products that partition to aerosol phase, were formed in the aqueous phase and caused the increasing of ratio of m/z 44 to m/z 43.

Different properties of SOA were observed in experiments with the two sulfate seed particles under different RHs. In Fig. 3(b), with 50% RH, the ratio of m/z 44 to m/z 43 (degree of oxidation) for experiment using $FeSO_4$ seed particles is much higher than that with $(NH_4)_2SO_4$ seed particles. Although the oxidation degree increase continuously over the experiment with the $(NH_4)_2SO_4$ seed particles, the final ratio of m/z 44 to m/z 43 remains much lower than that in the experiment with the $FeSO_4$ seed particles. However, at 12% RH, time variations of the ratio of the m/z 44 to m/z 43 are similar in the experiment with $FeSO_4$ or $(NH_4)_2SO_4$ seed particles.

The oxidation state of SOA is related to RH. In experiments with the $FeSO_4$ seed particles, the ratio of m/z 44 to m/z 43 is always lower in experiments with 12% RH than that with 50% RH. In other words, at RH = 50%, the degree of oxidation of SOA on the $FeSO_4$ seed particles was higher than at lower RH. Combined with the reduction of SOA formation on the $FeSO_4$ seed particles at the higher RH, this indicates that faster oxidation takes place in aqueous phase than that in dry condition. In the two experiments with the $(NH_4)_2SO_4$ seed particles, the minimum values for the ratio of m/z 44 to m/z 43 are similar, indicating the initially partitioned SOA from gas phase reaction have similar oxidation degree

regardless of the RHs. However, as reaction continued, the ratio of m/z 44 to m/z 43 increases more quickly in experiments at 50% RH than at 12% RH. This may also be related to absorbed water on the $(NH_4)_2SO_4$ seed particles; although $(NH_4)_2SO_4$ particles do not deliquesce at 50% RH, their hygroscopic growth can still add significant amounts of water onto the particles, and mixed organic and inorganic were found to deliquesce at RH below the ones of the pure particles (Marcolli et al., 2004; Meyer et al., 2009). The water would help increasing the particle volume and hence enhance the total SOA dissolution in the seed particles. Dissolution of organics was reported as the driving process bringing organics into sulfate particles (Li et al., 2011). However, decreased SOA formation on the $FeSO_4$ seed particles was observed in experiments at 50% RH compare to that at 12% RH. This clearly demonstrated the decreasing effect of $FeSO_4$ seed particles on SOA mass.

The SOA formation and the oxidation processes in the aqueous phase are closely related. In the experiments with the $(NH_4)_2SO_4$ seed particles, both the SOA concentration and its degree of oxidation increased more quickly in the experiment at 50% RH than at 12% RH. While in the experiments with the $FeSO_4$ seed particles, a higher degree of oxidation but accompanied by a significantly lower mass of SOA was observed in the experiment at 50% RH than at 12% RH. Meanwhile, in the experiment with the $FeSO_4$ seed particles at 50% RH, the minimum value for the ratio of m/z 44 to m/z 43 was much higher than in the other experiments. The ratio further increased to 1.9 in less than 1.5 h and then remained essentially constant. It seems that the oxidation process in experiments with $FeSO_4$ seed particles at 50% RH is fast, and is different from on $(NH_4)_2SO_4$ seed particles. During oxidation, fragmentation and functionalization are competitive reactions which influence the loading of organic aerosol mass on the seed particles (Kroll et al., 2009). In experiments in the presence of the $FeSO_4$ seed particles at RH 50%, a lower organic mass with higher oxidized products indicates that fragmentation dominates, resulting in highly volatile small molecules. As mentioned earlier, we suspect that the decreasing effect of $FeSO_4$ seed particles is more likely due to liquid phase reactions in which Fe(II) and Fe(III) recycle leading to OH radical generation in the liquid phase (Deguillaume et al., 2005). The liquid phase OH radical thus enhances the SOA oxidation in the liquid phase and leading to a higher degree of oxidation, which is consistent with our observation.

4. Conclusions

Using smog chambers, the present study investigated the effects of $FeSO_4$ seed particles on SOA formation at different relative humidities in the α-pinene/NO_x and α-pinene/HONO photooxidation systems. The results indicate that $FeSO_4$ seed particles decrease SOA mass as long as water was present on the seed particle surface, but have no decreasing effect on SOA mass under dryer conditions at 12% RH. In comparison to $(NH_4)_2SO_4$ seed particles, higher oxidation level of SOA was observed in the surface layer of water on the $FeSO_4$ seed particles. The decreasing effect of $FeSO_4$ seed particles on the SOA mass is proposed to be related to oxidation processes in the surface layer of water. Free radicals, including OH, can be formed from catalytic cycling of Fe^{2+} and Fe^{3+} in the aqueous phase. These radicals can react further with the organic products of α-pinene oxidation on the seed particles. The oxidation may lead to formation of smaller molecules which have higher saturation vapor pressures and favor repartitioning to the gas phase, and therefore, reduces SOA mass.

Acknowledgments

This work was supported by the “Strategic Priority Research Program” of the Chinese Academy of Sciences (XDB05010300, XDB05010102) and the special fund of State Key Joint Laboratory of Environment Simulation and Pollution Control (14Z04ESPCR, 14K04ESPCT). This work was also financially and technically supported by Toyota Motor Corporation and Toyota Central Research and Development Laboratories Inc. Studies performed at the Environment Canada's 9 m^3 chamber were supported in part by Environment Canada's Clean Air Regulatory Agenda (CARA) Science Program.

References

Bunce, N.J., Liu, L., Zhu, J., Lane, D.A., 1997. Reaction of naphthalene and its derivatives with hydroxyl radicals in the gas phase. Environ. Sci. Technol. 31, 2252–2259.
Cakmak, S., Dales, R., Kauri, L.M., Mahmud, M., Van Ryswyk, K., Vanos, J., Liu, L., Kumarathasan, P., Thomson, E., Vincent, R., Weichenthal, S., 2014. Metal composition of fine particulate air pollution and acute changes in cardiorespiratory physiology. Environ. Pollut. 189, 208–214.
Cheng, S.H., Yang, L.X., Zhou, X.H., Xue, L.K., Gao, X.M., Zhou, Y., Wang, W.X., 2011. Size-fractionated water-soluble ions, situ pH and water content in aerosol on hazy days and the influences on visibility impairment in Jinan, China. Atmos. Environ. 45, 4631–4640.
Chu, B., Hao, J., Li, J., Takekawa, H., Wang, K., Jiang, J., 2013. Effects of two transition metal sulfate salts on secondary organic aerosol formation in toluene/NOx photooxidation. Front. Environ. Sci. Eng. 7, 1–9.
Chu, B., Hao, J., Takekawa, H., Li, J., Wang, K., Jiang, J., 2012. The remarkable effect of $FeSO_4$ seed aerosols on secondary organic aerosol formation from photooxidation of α-pinene/NOx and toluene/NOx. Atmos. Environ. 55, 26–34.
Chu, B., Wang, K., Takekawa, H., Li, J., Zhou, W., Jiang, J., Ma, Q., He, H., Hao, J., 2014. Hygroscopicity of particles generated from photooxidation of α-pinene under different oxidation conditions in the presence of sulfate seed aerosols. J. Environ. Sci. 26, 129–139.
Czoschke, N.M., Jang, M., Kamens, R.M., 2003. Effect of acidic seed on biogenic secondary organic aerosol growth. Atmos. Environ. 37, 4287–4299.
Deguillaume, L., Leriche, M., Desboeufs, K., Mailhot, G., George, C., Chaumerliac, N., 2005. Transition metals in atmospheric liquid phases: sources, reactivity, and sensitive parameters. Chem. Rev. 105, 3388–3431.
Ervens, B., George, C., Williams, J.E., Buxton, G.V., Salmon, G.A., Bydder, M., Wilkinson, F., Dentener, F., Mirabel, P., Wolke, R., Herrmann, H., 2003. CAPRAM 2.4 (MODAC mechanism): an extended and condensed tropospheric aqueous phase mechanism and its application. J. Geophys. Res.-Atmos. 108, 4426.
Ervens, B., Turpin, B.J., Weber, R.J., 2011. Secondary organic aerosol formation in cloud droplets and aqueous particles (aqSOA): a review of laboratory, field and model studies. Atmos. Chem. Phys. 11, 11069–11102.
Faust, B.C., Hoigne, J., 1990. Photolysis of Fe(III)-hydroxy complexes as sources of OH radicals in clouds, fog and rain. Atmos. Environ. Part A-Gen. Top. 24, 79–89.
Hallquist, M., Wenger, J.C., Baltensperger, U., Rudich, Y., Simpson, D., Claeys, M., Dommen, J., Donahue, N.M., George, C., Goldstein, A.H., Hamilton, J.F., Herrmann, H., Hoffmann, T., Iinuma, Y., Jang, M., Jenkin, M.E., Jimenez, J.L., Kiendler-Scharr, A., Maenhaut, W., McFiggans, G., Mentel, T.F., Monod, A., Prevot, A.S.H., Seinfeld, J.H., Surratt, J.D., Szmigielski, R., Wildt, J., 2009. The formation, properties and impact of secondary organic aerosol: current and emerging issues. Atmos. Chem. Phys. 9, 5155–5236.
He, K.B., Yang, F.M., Ma, Y.L., Zhang, Q., Yao, X.H., Chan, C.K., Cadle, S., Chan, T., Mulawa, P., 2001. The characteristics of PM2.5 in Beijing, China. Atmos. Environ. 35, 4959–4970.
Healy, R.M., Temime, B., Kuprovskyte, K., Wenger, J.C., 2009. Effect of relative humidity on gas/particle partitioning and aerosol mass yield in the photooxidation of p-Xylene. Environ. Sci. Technol. 43, 1884–1889.
Hessberg, C.v., Hessberg, P.v., Poschl, U., Bilde, M., Nielsen, O.J., Moortgat, G.K., 2009. Temperature and humidity dependence of secondary organic aerosol yield from the ozonolysis of beta-pinene. Atmos. Chem. Phys. 9, 3583–3599.
Jang, M.S., Czoschke, N.M., Lee, S., Kamens, R.M., 2002. Heterogeneous atmospheric aerosol production by acid-catalyzed particle-phase reactions. Science 298, 814–817.
Jonsson, A.M., Hallquist, M., Ljungstrom, E., 2008. The effect of temperature and water on secondary organic aerosol formation from ozonolysis of limonene, Delta(3)-carene and alpha-pinene. Atmos. Chem. Phys. 8, 6541–6549.
Kaiser, J., 2005. How dirty air hurts the heart. Science 307, 1858–1859.
Kroll, J.H., Chan, A.W.H., Ng, N.L., Flagan, R.C., Seinfeld, J.H., 2007. Reactions of semivolatile organics and their effects on secondary organic aerosol formation. Environ. Sci. Technol. 41, 3545–3550.
Kroll, J.H., Smith, J.D., Che, D.L., Kessler, S.H., Worsnop, D.R., Wilson, K.R., 2009. Measurement of fragmentation and functionalization pathways in the heterogeneous oxidation of oxidized organic aerosol. Phys. Chem. Chem. Phys. 11, 8005–8014.
Li, S.M., Liggio, J., Graham, L., Lu, G., Brook, J., Stroud, C., Zhang, J., Makar, P., Moran, M.D., 2011. Condensational uptake of semivolatile organic compounds in gasoline engine exhaust onto pre-existing inorganic particles. Atmos. Chem. Phys. 11, 10157–10171.
Liggio, J., Li, S.-M., Vlasenko, A., Sjostedt, S., Chang, R., Shantz, N., Abbatt, J., Slowik, J.G., Bottenheim, J.W., Brickell, P.C., Stroud, C., Leaitch, W.R., 2010.

Primary and secondary organic aerosols in urban air masses intercepted at a rural site. J. Geophys. Res.-Atmos. 115.
Liggio, J., Li, S.M., 2008. Reversible and irreversible processing of biogenic olefins on acidic aerosols. Atmospheric Chem. Phys. 8, 2039–2055.
Liggio, J., Li, S.M., 2013. A new source of oxygenated organic aerosol and oligomers. Atmospheric Chem. Phys. 13, 2989–3002.
Liggio, J., Li, S.M., Brook, J.R., Mihele, C., 2007. Direct polymerization of isoprene and alpha-pinene on acidic aerosols. Geophys. Res. Lett. 34.
Liggio, J., Li, S.M., McLaren, R., 2005. Heterogeneous reactions of glyoxal on particulate matter: identification of acetals and sulfate esters. Environ. Sci. Technol. 39, 1532–1541.
Liu, C., Chu, B., Liu, Y., Ma, Q., Ma, J., He, H., Li, J., Hao, J., 2013. Effect of mineral dust on secondary organic aerosol yield and aerosol size in α-pinene/NOx photooxidation. Atmospheric Environ. 77, 781–789.
Liu, X.Y., Zhang, W.J., Huang, M.Q., Wang, Z.Y., Hao, L.Q., Zhao, W.W., 2009. Effect of illumination intensity and light application time on secondary organic aerosol formation from the photooxidation of alpha-pinene. J. Environ. Sci.-China 21, 447–451.
Lu, Z.F., Hao, J.M., Li, J.H., Wu, S., 2008. Effect of calcium sulfate and ammonium sulfate aerosol on secondary organic aerosol formation. Acta Chim. Sin. 66, 419–423.
Lu, Z.F., Hao, J.M., Takekawa, H., Hu, L.H., Li, J.H., 2009. Effect of high concentrations of inorganic seed aerosols on secondary organic aerosol formation in the m-xylene/NOx photooxidation system. Atmospheric Environ. 43, 897–904.
Marcolli, C., Luo, B.P., Peter, T., 2004. Mixing of the organic aerosol fractions: liquids as the thermodynamically stable phases. J. Phys. Chem. 108, 2216–2224.
Meyer, N.K., Duplissy, J., Gysel, M., Metzger, A., Dommen, J., Weingartner, E., Alfarra, M.R., Prevot, A.S.H., Fletcher, C., Good, N., McFiggans, G., Jonsson, A.M., Hallquist, M., Baltensperger, U., Ristovski, Z.D., 2009. Analysis of the hygroscopic and volatile properties of ammonium sulphate seeded and unseeded SOA particles. Atmos. Chem. Phys. 9, 721–732.
Ng, N.L., Canagaratna, M.R., Zhang, Q., Jimenez, J.L., Tian, J., Ulbrich, I.M., Kroll, J.H., Docherty, K.S., Chhabra, P.S., Bahreini, R., Murphy, S.M., Seinfeld, J.H., Hildebrandt, L., Donahue, N.M., DeCarlo, P.F., Lanz, V.A., Prévôt, A.S.H., Dinar, E., Rudich, Y., Worsnop, D.R., 2010. Organic aerosol components observed in Northern Hemispheric datasets from aerosol mass spectrometry. Atmos. Chem. Phys. 10, 4625–4641.
Nguyen, T.B., Roach, P.J., Laskin, J., Laskin, A., Nizkorodov, S.A., 2011. Effect of humidity on the composition of isoprene photooxidation secondary organic aerosol. Atmos. Chem. Phys. 11, 6931–6944.
Oakes, M., Rastogi, N., Majestic, B.J., Shafer, M., Schauer, J.J., Edgerton, E.S., Weber, R.J., 2010. Characterization of soluble iron in urban aerosols using near-real time data. J. Geophys. Res.-Atmos. 115, D15302.
Odum, J.R., Hoffmann, T., Bowman, F., Collins, D., Flagan, R.C., Seinfeld, J.H., 1996. Gas/particle partitioning and secondary organic aerosol yields. Environ. Sci. Technol. 30, 2580–2585.
Pandis, S.N., Harley, R.A., Cass, G.R., Seinfeld, J.H., 1992. Secondary organic aerosol formation and transport. Atmospheric Environ. Part A-Gen. Top. 26, 2269–2282.
Prisle, N.L., Engelhart, G.J., Bilde, M., Donahue, N.M., 2010. Humidity influence on gas-particle phase partitioning of alpha-pinene + O_3 secondary organic aerosol. Geophys. Res. Lett. 37, L01802.
Qi, L., Nakao, S., Tang, P., Cocker, D.R., 2010. Temperature effect on physical and chemical properties of secondary organic aerosol from m-xylene photooxidation. Atmospheric Chem. Phys. 10, 3847–3854.
Roberts, J.M., Veres, P., Warneke, C., Neuman, J.A., Washenfelder, R.A., Brown, S.S., Baasandorj, M., Burkholder, J.B., Burling, I.R., Johnson, T.J., Yokelson, R.J., de Gouw, J., 2010. Measurement of HONO, HNCO, and other inorganic acids by negative-ion proton-transfer chemical-ionization mass spectrometry (NI-PT-CIMS): application to biomass burning emissions. Atmos. Meas. Tech. 3, 981–990.
Satheesh, S.K., Moorthy, K.K., 2005. Radiative effects of natural aerosols: a review. Atmos. Environ. 39, 2089–2110.
Song, C., Na, K.S., Cocker, D.R., 2005. Impact of the hydrocarbon to NOx ratio on secondary organic aerosol formation. Environ. Sci. Technol. 39, 3143–3149.
Takekawa, H., Minoura, H., Yamazaki, S., 2003. Temperature dependence of secondary organic aerosol formation by photo-oxidation of hydrocarbons. Atmospheric Environ. 37, 3413–3424.
Tao, F., Gonzalez-Flecha, B., Kobzik, L., 2003. Reactive oxygen species in pulmonary inflammation by ambient particulates. Free Radic. Biol. Med. 35, 327–340.
Tillmann, R., Hallquist, M., Jonsson, A.M., Kiendler-Scharr, A., Saathoff, H., Iinuma, Y., Mentel, T.F., 2010. Influence of relative humidity and temperature on the production of pinonaldehyde and OH radicals from the ozonolysis of alpha-pinene. Atmospheric Chem. Phys. 10, 7057–7072.
Veres, P., Roberts, J.M., Warneke, C., Welsh-Bon, D., Zahniser, M., Herndon, S., Fall, R., de Gouw, J., 2008. Development of negative-ion proton-transfer chemical-ionization mass spectrometry (NI-PT-CIMS) for the measurement of gas-phase organic acids in the atmosphere. Int. J. Mass Spectrom. 274, 48–55.
Verheggen, B., Mozurkewich, M., Caffrey, P., Frick, G., Hoppel, W., Sullivan, W., 2007. alpha-Pinene oxidation in the presence of seed aerosol: estimates of nucleation rates, growth rates, and yield. Environ. Sci. Technol. 41, 6046–6051.
Vidrio, E., Jung, H., Anastasio, C., 2008. Generation of hydroxyl radicals from dissolved transition metals in surrogate lung fluid solutions. Atmospheric Environ. 42, 4369–4379.
Warren, B., Song, C., Cocker, D.R., 2008. Light intensity and light source influence on secondary organic aerosol formation for the m-xylene/NOx photooxidation system. Environ. Sci. Technol. 42, 5461–5466.
Wu, S., Lu, Z.F., Hao, J.M., Zhao, Z., Li, J.H., Hideto, T., Hiroaki, M., Akio, Y., 2007. Construction and characterization of an atmospheric simulation smog chamber. Adv. Atmos. Sci. 24, 250–258.
Zhang, H., Surratt, J.D., Lin, Y.H., Bapat, J., Kamens, R.M., 2011. Effect of relative humidity on SOA formation from isoprene/NO photooxidation: enhancement of 2-methylglyceric acid and its corresponding oligoesters under dry conditions. Atmospheric Chem. Phys. 11, 6411–6424.
Zhang, Y.X., Schauer, J.J., Shafer, M.M., Hannigan, M.P., Dutton, S.J., 2008. Source apportionment of in vitro reactive oxygen species bioassay activity from atmospheric particulate matter. Environ. Sci. Technol. 42, 7502–7509.
Zhao, Z., Hao, J.M., Li, J.H., Wu, S., 2008. Second organic aerosol formation by irradiation of alpha-pinene-NOx-H_2O in an indoor smog chamber for atmospheric chemistry and physics. Chin. Sci. Bull. 53, 3294–3300.
Zhuang, G.S., Yi, Z., Duce, R.A., Brown, P.R., 1992. Link between iron and sulphur cycles suggested by detection of Fe(II) in remote marine aerosols. Nature 355, 537–539.